

# Genetically engineering glycolysis in T cells increases their antitumor function

Raphaëlle Toledano Zur,<sup>1</sup> Orna Atar,<sup>2</sup> Tilda Barliya,<sup>1</sup> Shiran Hoogi,<sup>1</sup> Ifat Abramovich,<sup>2</sup> Eyal Gottlieb,<sup>2</sup> Noga Ron-Harel,<sup>2</sup> Cyrille J Cohen <sup>3</sup>

**To cite:** Toledano Zur R, Atar O, Barliya T, *et al.* Genetically engineering glycolysis in T cells increases their antitumor function. *Journal for ImmunoTherapy of Cancer* 2024;**12**:e008434. doi:10.1136/jitc-2023-008434

► Additional supplemental material is published online only. To view, please visit the journal online (<https://doi.org/10.1136/jitc-2023-008434>).

Accepted 20 May 2024

## ABSTRACT

**Background** T cells play a central role in the antitumor response. However, they often face numerous hurdles in the tumor microenvironment, including the scarcity of available essential metabolites such as glucose and amino acids. Moreover, cancer cells can monopolize these resources to thrive and proliferate by upregulating metabolite transporters and maintaining a high metabolic rate, thereby outcompeting T cells.

**Methods** Herein, we sought to improve T-cell antitumor function in the tumor vicinity by enhancing their glycolytic capacity to better compete with tumor cells. To achieve this, we engineered human T cells to express a key glycolysis enzyme, phosphofructokinase, in conjunction with Glucose transporter 3, a glucose transporter. We co-expressed these, along with tumor-specific chimeric antigen or T-cell receptors.

**Results** Engineered cells demonstrated an increased cytokine secretion and upregulation of T-cell activation markers compared with control cells. Moreover, they displayed superior glycolytic capacity, which translated into an improved in vivo therapeutic potential in a xenograft model of human tumors.

**Conclusion** In summary, these findings support the implementation of T-cell metabolic engineering to enhance the efficacy of cellular immunotherapies for cancer.

## BACKGROUND

A large body of studies in humans and mice has established that CD8<sup>+</sup> T cells can control tumor progression.<sup>1</sup> Different approaches have been identified during the last decade to enhance antitumor immunity.<sup>2</sup> These approaches include mainly the use of immune checkpoint inhibitors<sup>3</sup> and the adoptive cell transfer of tumor-reactive T cells.<sup>4</sup> The latter may be either expanded from tumor-infiltrating lymphocytes (TILs) or genetically engineered to express T-cell receptors (TCR) or chimeric antigen receptors (CAR) specific to a tumor antigen.<sup>5</sup> Notably, the CAR therapy approach demonstrates encouraging results for hematological malignancies treatment, as we and others demonstrated.<sup>6–9</sup> However, efficient antitumor immune responses can be dampened by different mechanisms, such as tumor-induced immunosuppression and metabolic dysfunction. For example,

## WHAT IS ALREADY KNOWN ON THIS TOPIC

⇒ T cells in the tumor microenvironment face critical metabolic requirements and must compete for essential resources with tumors, which often exhibit high glycolytic activity.

## WHAT THIS STUDY ADDS

⇒ This study aimed to investigate whether enhancing glycolysis could improve the therapeutic outcomes of T-cell receptor or chimeric antigen receptor-engineered T cells. Our findings demonstrate that co-expressing key glucose metabolism components, specifically phosphofructokinase and glucose transporter 3, in engineered T cells leads to superior antitumor function both in vitro and, more importantly, in a xenograft model using NSG mice and human melanoma tumors.

## HOW THIS STUDY MIGHT AFFECT RESEARCH, PRACTICE OR POLICY

⇒ These results have the potential to significantly enhance the development of more efficient cellular immunotherapies for cancer.

acidification, hypoxia, lack of glucose, and the accumulation of immunosuppressive metabolites in the tumor microenvironment (TME) negatively affect T cells, leading to hypofunction and cellular death.<sup>7–10</sup> T cells often lack access to essential nutrients required to thrive or exert effector functions when mounting a response to tumor cells.<sup>8</sup> The latter can undergo metabolic changes that allow for increased nutrient uptake and pathway rewiring that favor their growth, as in the “Warburg effect”.

Glucose is a central nutrient that all cells metabolize to produce energy during rapid growth. In glycolysis, one glucose molecule is converted through a 10-step enzymatic process into two pyruvate molecules, either used for aerobic respiration and oxidative phosphorylation in the mitochondria or further converted into lactate during aerobic glycolysis. Importantly, augmented glucose metabolism on T-cell activation is critical for the rapid onset of proliferation through



© Author(s) (or their employer(s)) 2024. Re-use permitted under CC BY-NC. No commercial re-use. See rights and permissions. Published by BMJ.

<sup>1</sup>Bar-Ilan University, Ramat Gan, Israel

<sup>2</sup>Technion Israel Institute of Technology, Haifa, Haifa, Israel

<sup>3</sup>Faculty of Life Sciences, Bar-Ilan University, Ramat Gan, Tel Aviv, Israel

## Correspondence to

Professor Cyrille J Cohen; [cyrille.cohen@biu.ac.il](mailto:cyrille.cohen@biu.ac.il)

the synthesis of metabolites.<sup>11</sup> In T cells, glycolysis is also critical to producing key effector molecules like interferon (IFN)- $\gamma$ .<sup>12</sup> Glycolytic metabolites such as phosphoenolpyruvate may act as a checkpoint and facilitate T-cell activation.<sup>13</sup>

Following activation, T cells upregulate the expression of glucose transporters (eg, GLUT1 and GLUT3) and glycolytic enzymes,<sup>14</sup> while continuing using aerobic respiration to produce ATP necessary for their activity and proliferation.<sup>13</sup> One of the glycolysis enzymatic components, phosphofruktokinase (PFK), is a rate-limiting enzyme that catalyzes the conversion of fructose 6-phosphate to fructose 1,6-bisphosphate (F1,6BP) and can regulate glycolysis through allosteric inhibition or activation.<sup>15</sup> More specifically, F1,6BP regulates glycolysis primarily by activating the enzyme PFK, a crucial step in the glycolytic pathway. This activation accelerates glycolysis, directing glucose toward energy production. Essentially, F1,6BP acts as a signal for the cell to increase its energy production when needed.<sup>15</sup> The enzyme activity depends on the ATP/AMP ratio and may display lower activity at acidic pH, as observed in the TME.<sup>16,17</sup>

In the present study, we aimed to improve T-cell anti-tumor function by genetically manipulating the glycolysis pathway. We focused on PFK since it is a key regulatory, rate-limiting enzyme in glycolysis playing a pivotal role in controlling the overall glycolytic flux and being the first enzyme unique to the glycolytic pathway. We used the forced expression of PFK to improve glycolysis rate and ATP production in T cells. Then, to increase the glucose influx, we assessed the feasibility of expressing the high-affinity glucose transporter GLUT3 in T cells. Finally, we combined both PFK and GLUT3 and showed that this strategy could improve antitumor function *in vitro*, but importantly also in a xenograft model of human tumors.

## METHODS

### Peripheral blood mononuclear cells and cell lines

Peripheral blood mononuclear cells (PBMCs) were obtained from healthy donors from the Israeli Blood Bank (Tel-Hashomer, Israel). Melanoma cell lines HLA-A2<sup>+</sup>/MART-1<sup>+</sup> (624.38) and HLA-A2<sup>-</sup>/MART-1<sup>+</sup> (888) were generated at the Surgery Branch (National Cancer Institute, National Institutes of Health, Bethesda, Maryland, USA), as described previously.<sup>18</sup> 888A2 is an HLA-A2-transduced line derived from 888. SK-MEL23 is an HLA-A2<sup>+</sup> melanoma cell line (CVCL\_6027). 888, SK-MEL23 and 624.38 were reported to be MART-1<sup>+</sup>.<sup>19</sup> A375 (CVCL\_0132) melanoma is HLA-A2<sup>+</sup>/MART-1<sup>-</sup>. Adherent cells were cultured in DMEM (Invitrogen, Carlsbad, California, USA), supplemented with 10% heat-inactivated fetal bovine serum (Biological Industries, Beth Haemek, Israel). K562 (CCL\_243) was engineered to express the CD19 antigen by retroviral transduction. Non-adherent tumor cells were cultured in RPMI (Invitrogen, Carlsbad, California, USA), supplemented with 10% heat-inactivated fetal bovine serum (Biological

Industries, Beth Haemek, Israel). Human lymphocytes were cultured in BioTarget medium (Biological Industries, Beth Haemek, Israel), supplemented with 10% heat-inactivated fetal bovine serum (FBS) and 300 IU/mL IL-2 (PeproTech, Israel). All cells were maintained at 37°C and 5% CO<sub>2</sub>.

### Transduction of PBLs and retroviral constructs

Retroviral transduction was performed as previously described using RetroNectin (Takara, Japan).<sup>18,20</sup> The  $\alpha$  and  $\beta$  chains from the previously characterized MART-1-specific TCR were subcloned into the MSGV1 vector, as described.<sup>18</sup> As a control or reporter gene, we used a truncated version of nerve growth factor receptor (NGFR).<sup>18</sup> The complementary DNA (cDNA) encoding PFK and GLUT3 were purchased (SinoBiological, Houston, Texas, USA) and subcloned into the MSGV1 vector. Freshly isolated peripheral blood lymphocytes (PBLs) were stimulated in the presence of 50 ng/mL OKT3 (eBioscience, San Diego, California, USA). 2 days after stimulation, lymphocytes were transduced consecutively, first with a TCR or CAR, and after 24 hours, with viral supernatant encoding the metabolic genes or control.

### Gene-expression analysis by real-time PCR

Messenger RNA (mRNA) was extracted according to the manufacturer's instructions using the Total RNA Mini Kit (Geneaid, Taiwan). cDNA was synthesized using the iScript cDNA Synthesis kit (Bio-Rad, Israel). Real-time PCR was performed in triplicates with SYBR Green ER qPCR (Hylabs, Israel). RNA levels of each candidate gene, as quantified by the PCR system, were normalized to  $\beta$ -actin. The oligonucleotides used for quantitative PCR are as follows:  $\beta$ -actin (For: 5'-CTGTACGCCAACACAGTGCT-3' and Rev: 5'-GCTCAGGAGGCAATGATC-3'), PFK (For: 5'-TGCCCCTCATGGAATGTGTC-3' and Rev: 5'-ATACCGGGGTCTGACATGA-3') and GLUT3 (For: 5'-TGATCGGCTCCTTTCCGTC-3' and Rev: 5'-TCCCATAAAGCAGCCACCAG-3').

### Antibodies and flow cytometry

Fluorophore-labeled anti-human NGFR, CD8, CD4, CD137, TIM3, LAG3, TIGIT, PD-1, CD69, CD25, CCR7, CD45RO, CD107a and Streptavidin were purchased from BioLegend (San Diego, California, USA). Biotinylated Protein L (Thermo Fisher) was used to stain T cells for CAR expression as previously reported.<sup>21</sup> Cells were stained in phosphate-buffered saline (PBS), 0.5% bovine serum albumin (BSA), and 0.02% sodium azide for 30 min on ice. For intracellular staining, cells were fixed with pre-formaldehyde 4% and permeabilized using ice-cold 90% methanol for 20 min. Then, the cells were washed in PBS buffer and stained for anti-PFK antibody (EPR10734(B), Abcam). Proliferation assays using carboxyfluorescein succinimidyl ester (CFSE) were performed as previously described.<sup>18</sup> Cells were analyzed by flow cytometry, gated on the live population as described.

### Cytokine release and cytotoxicity assays

Lymphocyte cultures were tested for reactivity in cytokine release assays using commercially available human ELISA kits for interleukin (IL)-2, IFN- $\gamma$ , and tumor necrosis factor (TNF)- $\alpha$  (R&D Systems, Minneapolis, Minnesota, USA). For these assays,  $1 \times 10^5$  responder cells (T cells) and  $1 \times 10^5$  stimulator cells (tumor cells) were incubated for 16 hours in a 200  $\mu$ L culture volume in individual wells of 96-well plates. For cytotoxicity,  $1 \times 10^4$  mCherry expressing target cells were seeded on a flat 96 plate well and co-cultured with T cells at a ratio of 1:1 to 5:1 effector:target (E:T) for 36 hours in an IncuCyte apparatus and analyzed for orange integrated intensity of three to four replicates wells.

### Metabolism-related assays

Extracellular acidification rate using a Glycolysis Stress Test kit was measured from cells in non-buffered Dulbecco's Modified Eagle Medium (DMEM) containing 5 mM glucose, 2 mM L-glutamine, and 1 mM sodium pyruvate, under basal conditions in response to glycolysis inhibitors (glucose 11.1 mM, 1.15  $\mu$ M oligomycin, and 100 mM 2-DG—Sigma-Aldrich) on the SeaHorse XFe96 Extracellular Flux Analyzer (Agilent Technologies). Additionally, ECAR was measured using a Glycolysis Assay Kit (Abcam, #ab197244) according to the manufacturer's instructions. Lactate was analyzed using HPLC-MS after culturing T cells with <sup>13</sup>C6 labeled glucose added to glucose-free Roswell Park Memorial Institute (RPMI) medium for 30 min. Glucose uptake was measured using the Glucose Assay Kit (Abcam, #ab65333) following the manufacturer's instructions. Cellular ATP levels were measured using CellTiter-Glo 2.0 Cell Viability Assay, ATP measurement kit (Promega), according to the manufacturer's instructions.

### In vivo assay

NSG mice were inoculated with 2 million 888/A2 tumor cells in 100  $\mu$ L Hanks Balanced Salt Solution (HBSS) and 100  $\mu$ L Cultrex matrix (Trevigen), using an insulin syringe with a 27-gauge needle, in the dorsal flank of 6–12 weeks NSG mice. On tumor establishment, mice were randomized and injected in the tail vein with two injections of  $5 \times 10^6$  transduced lymphocytes on days 7 and 14 after tumor inoculation. There were no outliers. Tumor growth was measured every 2–3 days in a blinded fashion using a caliper and calculated using:  $D \times d^2 \times \pi / 6$ , where D is the largest tumor diameter and d is its perpendicular diameter. All the procedures were approved by the Bar-Ilan university committee for animal welfare under the Ministry of Health (#39-06-2019).

### Statistical analysis

A paired Student's log t-test was used to determine statistical significance. Data are reported as mean  $\pm$  SEM. Statistical values, including the number of replicates (n), can be found in the figure legends #p<0.1, \*p<0.05, \*\*p<0.01, \*\*\*p<0.001. Survival curves were compared using a

LogRank analysis. The statistical test used for each figure is described in the corresponding legend.

## RESULTS

### Human T cells can be engineered to express high levels of PFK

PFK is considered a glycolytic rate-limiting enzyme and essential for the commitment to glycolysis.<sup>17,22</sup> We aimed to determine if its forced expression might impact T-cell activity. To this end, we constructed a retroviral vector driving high expression levels of human PFK. Primary human T cells were transduced with PFK or truncated NGFR (control). We observed a high expression of NGFR truncated gene with a mean fluorescence intensity (MFI) of 359 compared with seven in untransduced T cells (figure 1A). A statistically significant increase was observed in PFK expression, with an MFI of 2,317 positive cells in the PFK-transduced population compared with 442 and 529 in the control groups (NGFR and untransduced T cells) (figure 1B). To confirm this, we evaluated the impact of PFK transduction at the RNA level by quantitative PCR. We observed close to a 10-fold increase in the levels of PFK mRNA transcript in transduced cells (figure 1C). We also followed the levels of PFK expression over time after transduction. We noted significantly higher levels of PFK expression up to 3–4 weeks compared with control NGFR-transduced or untransduced T cells (at day 23, MFI=2,473 vs 569 vs 521, respectively; figure 1D).

In parallel, we engineered T cells to concomitantly express a tumor-specific receptor to target cancer cells; we used either MART1-specific TCRs, as previously characterized,<sup>23</sup> or a CD19-specific CAR.<sup>24</sup> To negate any functional difference deriving from a differential TCR/CAR expression between the examined experimental groups, we first performed a TCR or CAR transduction step and then used these cells for subsequent transduction with PFK or the control gene (NGFR). We also carefully and constantly controlled for equal TCR/CAR expression following transduction. As depicted in figure 1E,F, we were able to express both receptors concomitantly with PFK in human T cells efficiently without any selection. As aforementioned, the levels of expression of TCR and CAR were similar between all tested groups and sustained for more than 30 days without selection (online supplemental figure 1A,B).

### PFK-engineered T cells exhibit improved glycolysis

Next, we phenotypically characterized the PFK-transduced population. We measured the distribution of CD4+/CD8+ cells following transduction. No statistically significant difference was shown between the PFK and control populations, with an approximate CD4/CD8 ratio of 25%/75%, respectively (figure 2A). Similarly, we also assessed the memory phenotype of transduced cells by staining them for CD45RO and CCR7 and dividing them into effector memory, central memory, EMRA (terminally differentiated effector memory cells re-expressing CD45RA), or naïve cell population. We noted



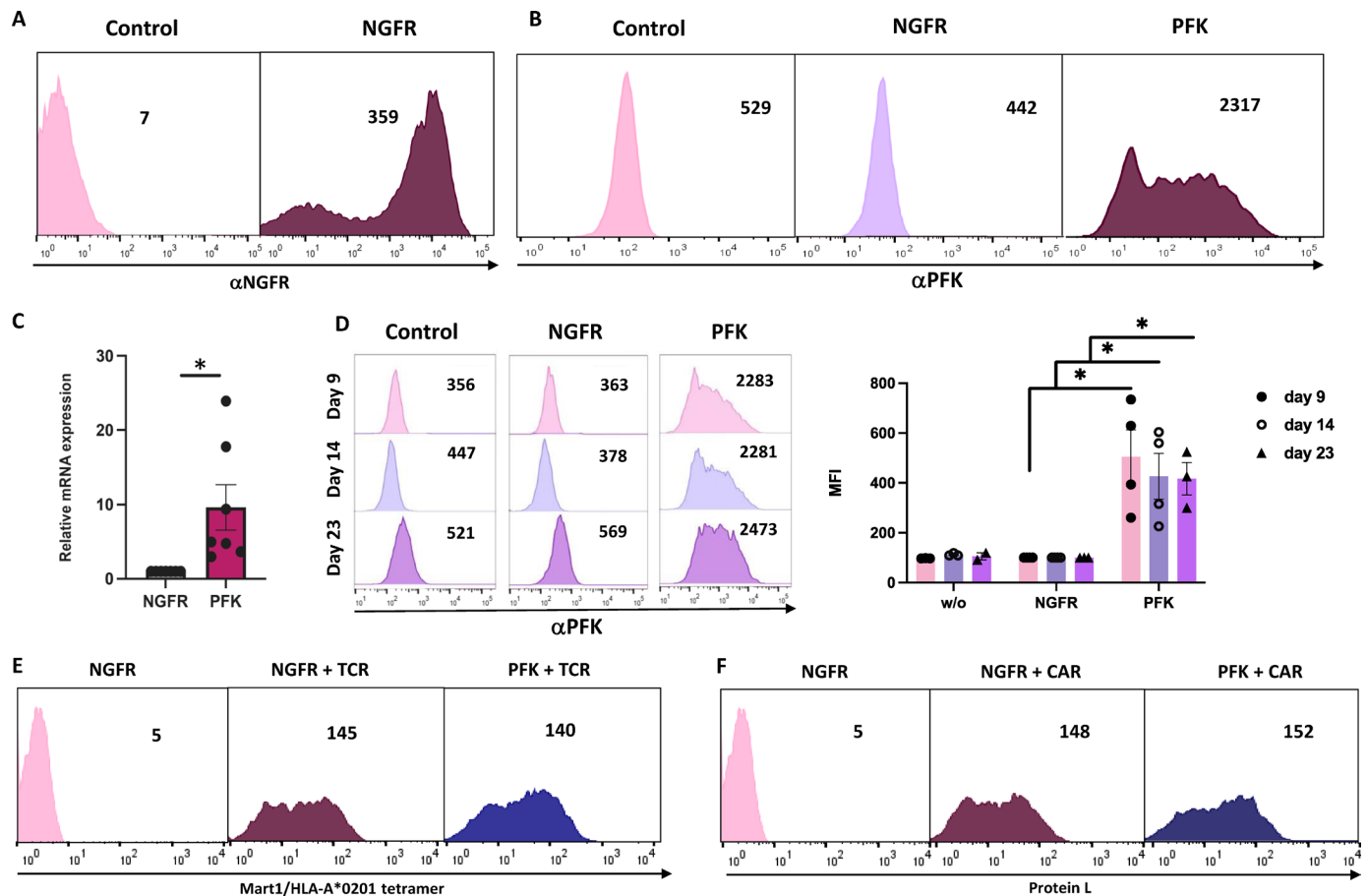


**Figure 1** Human T cells can be modified to express high levels of PFK. (A–B) Human PBLs were transduced with the retroviral vectors encoding the PFK or the NGFR gene (truncated NGFR). 72 hours after transduction, PFK or NGFR expression was measured by flow cytometry using antibodies specific for PFK ( $\alpha$ PFK) or NGFR ( $\alpha$ NGFR). These MFI results are representative of at least five independent experiments with at least five different donors. The difference between the population transduced with PFK and that transduced with NGFR was found statistically significant ( $*p < 0.05$ ; calculated using a Student's paired t-test). (C) RNA from T cells was extracted and reverse-transcribed after transduction with retroviral vectors encoding the PFK gene. PFK transcript expression was measured by quantitative PCR and normalized to that of the NGFR-transduced control. These results are presented as mean+SEM of 7 independent experiments performed with six different donors and were found statistically significant (as indicated, using a Student's paired t-test). (D) We measured PFK expression over time in untransduced PBLs (control), transduced PBLs with NGFR or with PFK. The MFI values of positive cells are shown for a representative experiment (left panel) and for three different experiments with three different donors (mean+SEM; right panel). The difference between PFK and NGFR groups was found statistically significant ( $*p < 0.05$  using a Student's paired t-test). (E–F) Human PBLs were transduced with an MART1-specific TCR (E) or a CD19-specific CAR (F). These results are representative of at least five independent experiments with at least five different donors. The difference between the CAR-transduced or TCR-transduced population and control was found statistically significant ( $*p < 0.05$ ; calculated using a Student's paired t-test). CAR, chimeric antigen receptor; MFI, mean fluorescence intensity; NGFR, nerve growth factor receptor; PBL, peripheral blood lymphocyte; PFK, phosphofruktokinase; TCR, T-cell receptor.

a significant difference in the distribution of the central memory population between PFK and control, with an average increase of approximately 45% in the PFK group (from 4.7% to 6.9% of total cells,  $p = 0.02$ ; [figure 2B](#)). Finally, we followed cell proliferation for 4 days (from d10 to d14 after transduction). A slight increase was observed in the proliferative capacity (with a proliferation factor based on an MFI ratio of 118 in the PFK group compared with 100 in the NGFR group;  $p < 0.01$ ) ([figure 2C](#)). To further understand the impact of PFK expression on engineered T cells, we measured the extracellular acidification rate (ECAR). PFK overexpression led to a significant increase in glycolysis compared with

NGFR control (an average of 80%;  $p < 0.01$ ) and glycolytic capacity (an average of 97%;  $p < 0.05$ ) but only a slight increase in glycolytic reserve (an average of 16%;  $p = 0.22$ ) ([figure 2D](#)). Moreover, we measured lactate levels using  $^{13}\text{C}$ -labeled glucose isotope tracing ([figure 2E,F](#)). PFK-transduced T cells demonstrated a significant increase in lactate (50% at m+3 [figure 2F](#);  $p < 0.05$ ). These results suggest that PFK-forced-expression T cells can lead to an increase in glycolysis, which may facilitate T-cell function. Overall, PFK-engineered cells demonstrated an increase in glycolysis and glycolytic capacity.

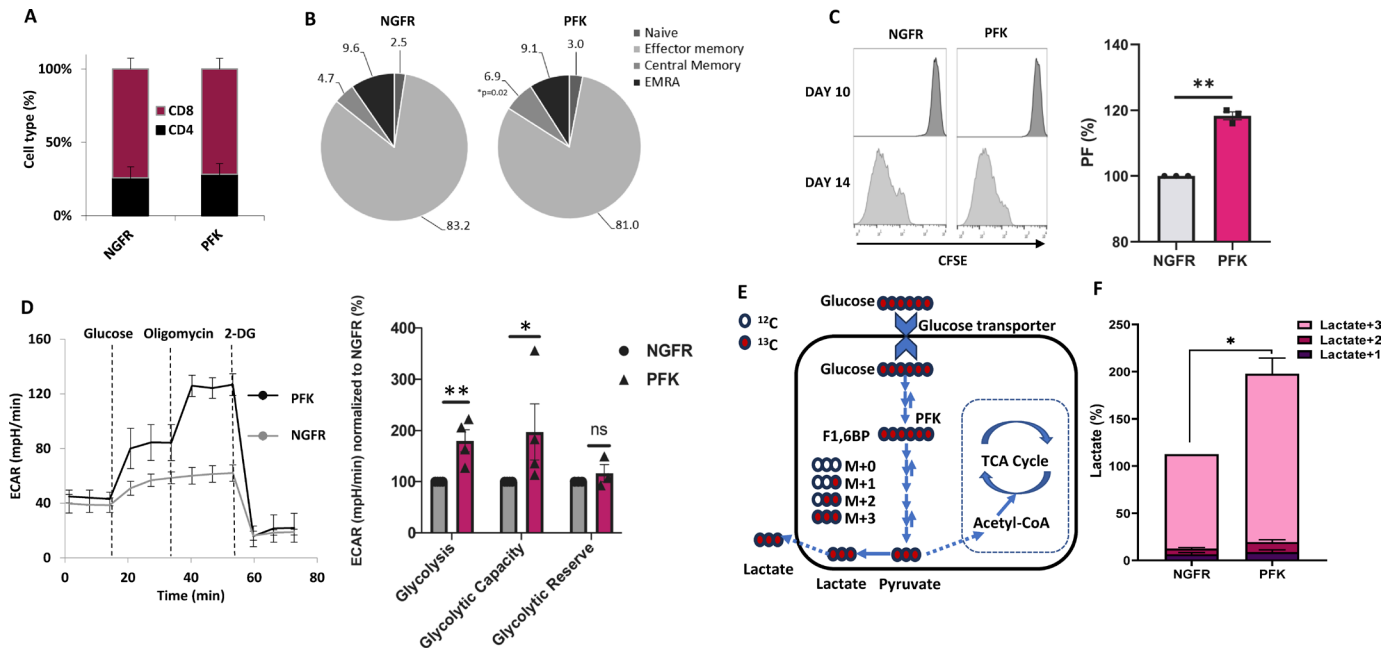


**Figure 2** PFK-engineered T cells exhibit improved glycolysis. (A) The CD4/CD8 ratio of transduced cells was determined by flow cytometry. These results are representative of eight independent experiments with four different donors. No significant difference was observed between the PFK and NGFR groups. (B) The memory phenotype of transduced cells was determined by flow cytometry based on CD45RO and CCR7 expression. EM—effector memory (CD45RO+/CCR7−), CM—central memory (CD45RO+/CCR7+), EMRA—terminally differentiated effector memory cells re-expressing CD45RA (CD45RO−/CCR7−) or naïve cell population (CD45RO+/CCR7+). These results are presented as the mean of 6 independent experiments with three different donors. The percentage of central memory cells was statistically significant between NGFR (control group) and PFK (\* $p < 0.05$ , using a Student's paired t-test). (C) T cells were labeled with CFSE and stimulated with anti-CD3 antibody for 4 days. The histograms of days 10 and 14 are shown in the left panel. In the right panel, the mean of the PF (proliferation factor=MFI day 10/MFI day 14 normalized to NGFR (control)) was calculated. These results are representative of three independent experiments performed with three different donors, found to be statistically significant (\*\* $p < 0.01$  using a Student's paired t-test). (D) Evaluation of T-cell metabolic function by the Seahorse extracellular flux analyzer. Extracellular acidification rate (ECAR) was measured. The left panel depicts a representative experiment ( $n = 8$  replicates). The right panel depicts the mean±SEM of 4 independent experiments performed with three donors, normalized to control NGFR (with an average value of 26.4, 50.8 and 31.4 mpH/min for the glycolysis, glycolytic capacity and reserve, respectively). The difference between the NGFR vector (control) and the PFK group was found statistically significant for the glycolysis rate and the glycolytic capacity as indicated (\*\* $p < 0.01$  and \* $p < 0.05$ , respectively, calculated using a Student's paired t-test). (E) Schematic representation of glucose fate mapping through glycolysis. A metabolite with  $n$  carbon atoms can have 0 to  $n$  of its carbon atoms labeled with  $^{13}\text{C}$ , resulting in isotopologues that increase in mass ( $M$ ) from  $M+0$  (all carbons unlabeled that is,  $^{12}\text{C}$ ) to  $M+n$  (all carbons labeled, that is,  $^{13}\text{C}$ ). (F) Lactate was measured by LC-MS following 30 min incubation with  $^{13}\text{C}_6$ -labeled glucose. The results were normalized to  $m+3$  and are presented as mean±SEM.  $n = 3$  different donors (\* $p < 0.05$  calculated using a Student's paired t-test).  $M$ =unlabeled mass of isotope;  $M+n$ =native metabolite mass ( $M$ )+number of isotopically labeled carbons ( $n$ ). CFSE, carboxyfluorescein succinimidyl ester; LC-MS, liquid chromatography-mass spectrometry; MFI, mean fluorescence intensity; NGFR, nerve growth factor receptor; PFK, phosphofructokinase.

### PFK-engineered T cells upregulate activation markers and display enhanced cytokine secretion

We then tested the biological activity of PFK-engineered T cells, which were stimulated with OKT3 and cultured overnight. PFK-engineered cells secreted significantly higher levels of TNF- $\alpha$ , IFN- $\gamma$ , and IL-2 compared with the control NGFR-transduced cells (figure 3A–C). When normalizing TNF- $\alpha$  secretion to that observed in the control group (100%—equivalent to an average of 5.3 ng/mL after stimulation), we observed an average increase of 70% ( $p < 0.01$ ) in the PFK group (figure 3A). Similarly, we observed superior secretion of IFN- $\gamma$  and IL-2 in T cells expressing PFK compared with the control group (eg, 36% and 43% more in the PFK group for IFN- $\gamma$  and

IL-2, respectively; figure 3B,C,  $p < 0.05$ ). Notably, no significant cytokine secretion was measured in unstimulated T cells. Altogether, PFK-expressing T cells demonstrated an improved cytokine secretion capability. The upregulation of activation markers, such as CD25, CD69, and 41BB (CD137), is an important factor that can enhance T-cell function. We assessed their surface expression on PFK-transduced or NGFR (control)-transduced T cells following OKT3-stimulation. Compared with the control T-cell population, PFK-engineered T cells demonstrated a statistically significant enhanced expression of these markers: for instance, for CD69, we detected an average of 40% of positive cells for PFK versus 32% for the control

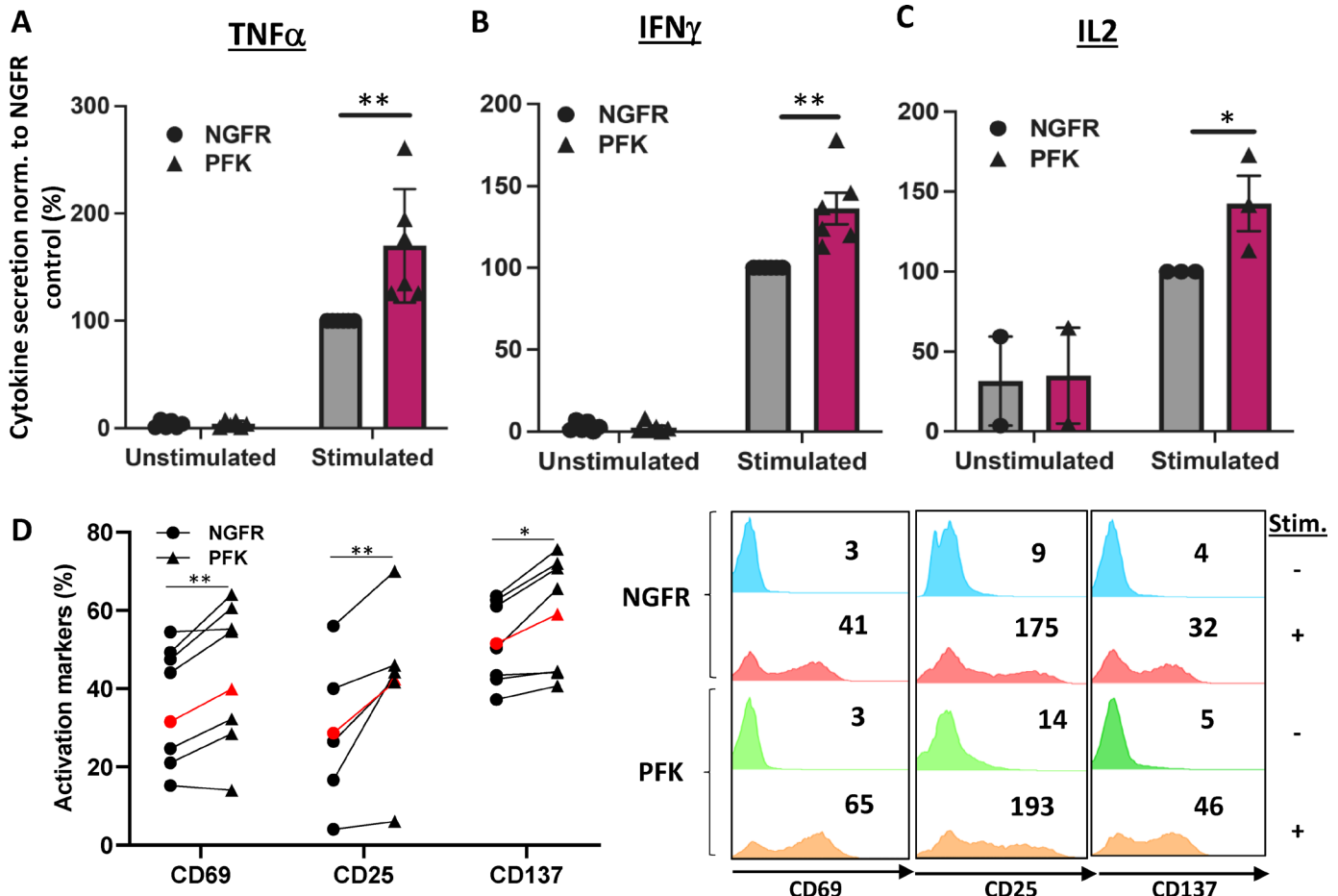


**Figure 3** PFK-engineered T cells upregulate activation markers and display enhanced cytokine secretion. (A–C) Primary human T cells were transduced with either NGFR vector (control) or PFK and were restimulated with plate-bound OKT3. TNF- $\alpha$  (A) IFN- $\gamma$  (B) and IL-2 (C) secreted in the culture supernatant were measured by ELISA. These results are the mean+SEM of at least three independent experiments performed with at least three different donors and normalized to control NGFR (with an average of 5.3, 7.45 and 0.365 ng/mL of TNF- $\alpha$ , IFN- $\gamma$  and IL-2, respectively). The difference between the PFK and the control group was found statistically significant as indicated (\* $p$ <0.05 or \*\* $p$ <0.01 calculated using a Student's paired t-test). (D) CD69, CD25, and CD137 expression were measured by flow cytometry, gated on the CD8<sup>+</sup> population. The left panel displays results from at least five independent experiments performed with at least three different donors. In the right panel, representative results for each group and each marker are shown. The first and third lines represent the unstimulated group, while the second and fourth lines represent the stimulated cells. Statistical significance between the PFK and control groups was determined (\* $p$ <0.05 or \*\* $p$ <0.01 calculated using a Student's paired t-test). IFN, interferon; IL, interleukin; NGFR, nerve growth factor receptor; PFK, phosphofructokinase; TNF, tumor necrosis factor.

(figure 3D;  $p$ =0.001). Similarly, we noted a proportion of 59% of positive cells for CD137 in the PFK sample compared with 52% in the control one and 57% versus 42% for CD25 (figure 3D).

#### PFK can enhance cytokine secretion in engineered T cells in co-cultures with tumor cells

T-cell specificity can be redirected against cancer by engineering them to express CARs or exogenous TCRs.<sup>4,5</sup> To assess the potential benefit of PFK in the context of a CAR expressing T-cell, we co-cultured PFK-engineered or NGFR-engineered  $\alpha$ CD19 CAR T cells with CD19-expressing targets (or antigen-negative K562 control). We observed in the co-culture with K562-CD19 an enhanced secretion of cytokines by the PFK-engineered group compared with the NGFR control, with an increase of

42% (normalized to control; 3.5 ng/mL) for TNF- $\alpha$ , 15% (normalized to control; 4 ng/mL) for IFN- $\gamma$ , and 28% (normalized to control; 1.3 ng/mL) for IL-2, ( $p$ <0.05) (figure 4A–C).

In addition to CAR T cells, we sought to examine if we could improve the function of T cells engineered to express a tumor-specific TCR. Primary human T cells were transduced to express an MART1-specific TCR and PFK (or NGFR, control). These cells were co-cultured with different human melanoma cell lines. We measured TNF- $\alpha$ , IFN- $\gamma$ , and IL-2 secretion (figure 4D–F). We noted a 1.3–2.5-fold increase in cytokine secretion in the PFK group with, for example, 241% more of TNF- $\alpha$ , 151% more of IFN- $\gamma$ , and 155% more of IL-2 in co-cultures with 624.38 (figure 3F). No significant cytokine secretion

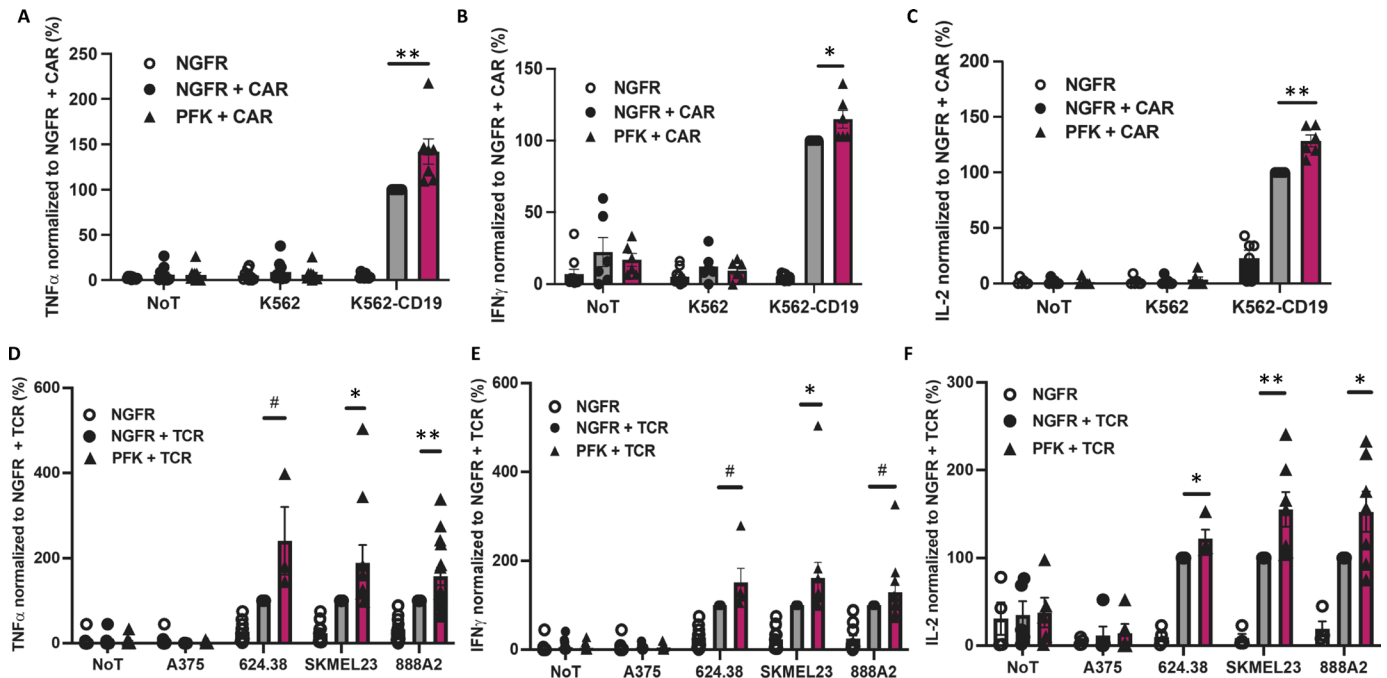


**Figure 4** PFK can enhance cytokine secretion in engineered T cells in co-cultures with tumor cells. (A–C) Primary human T cells were transduced with a CD19-CAR and either NGFR (control) or PFK. These cells were co-cultured with K562-CD19 (positive control) and K562 (negative control), or no target (NoT). TNF- $\alpha$  (A) IFN- $\gamma$  (B) and IL-2 (C) secreted in the co-culture supernatant were measured by ELISA. These results are represented as the mean+SEM of 4 independent experiments performed with three different donors. The results were normalized to the secretion in the NGFR+CAR group (with an average of 3.5, 4 and 1.3 ng/mL of TNF- $\alpha$ , IFN- $\gamma$  and IL-2, respectively). The difference between the NGFR vector (control) and PFK groups was found statistically significant as indicated (\*\* $p < 0.01$  and \* $p < 0.05$  calculated using a Student's paired t-test). (D–F) Transduced-PBLs expressing MART1-specific TCR receptor were co-cultured with 624.38, SKMEL23 and 888/A2 as positive controls and A375 cell line and no target (NoT) as negative control. TNF- $\alpha$  (D) IFN- $\gamma$  (E) and IL-2 (F) secreted in the co-culture supernatant were measured by ELISA. These results represent the mean+SEM of at least four independent experiments performed with at least three different donors. The results were normalized to NGFR+TCR (with reference concentrations ranging between 0.4 and 2.4 ng/mL for TNF- $\alpha$ , 0.6–5.9 ng/mL for IFN- $\gamma$  and 0.13 to 1.25 ng/mL for IL-2). The difference between NGFR vector (control) and PFK was found statistically significant as calculated using a Student's paired t-test. CAR, chimeric antigen receptor; IFN, interferon; IL, interleukin; NGFR, nerve growth factor receptor; PBL, peripheral blood lymphocyte; PFK, phosphofructokinase; TCR, T-cell receptor; TNF, tumor necrosis factor.

was observed in co-cultures with control A375 or in the absence of targets. Altogether, PFK-forced expression in T cells demonstrated an improved antitumor cytokine secretion capability.

### GLUT3 transporter-forced expression enhances glucose uptake, glycolysis and cytokine secretion by T cells

As aforementioned, reduced accessibility to nutrients such as glucose and competition with tumor cells can affect T cells' function, activation, and proliferation.<sup>8</sup> In that regard, tumors have been shown to often overexpress glucose transporters to enhance their glucose uptake capacity.<sup>25</sup> GLUT3 is a high-affinity glucose transporter, especially in comparison to GLUT1 (with a  $K_m$  2–3 vs 7–10 mM, respectively).<sup>26</sup> We hypothesized that improving glucose uptake by overexpressing GLUT3 transporter in human T cells could enhance their function.

We constructed a retroviral vector to overexpress GLUT3 linked by an IRES to a reporter gene (NGFR). As shown in [figure 5A,B](#), we successfully transduced primary human T cells with GLUT3-IRES-NGFR or NGFR only (control). We observed high transduction levels

(MFI=452 compared with control MFI=7) and confirmed this by real-time PCR analysis; on average, we noted 13 times more GLUT3 transcript expression in GLUT3-transduced cells than in control NGFR-engineered T cells ([figure 5B](#)).

To verify the hypothesis that GLUT3 can increase glucose uptake in T cells, we quantified glucose levels in the GLUT3-engineered T cells. We observed 51% increase in glucose level in the GLUT3 group compared with the control group ([figure 5C](#);  $p < 0.05$ ). We also observed in GLUT3-transduced cells a significant increase in glycolysis compared with NGFR control (an average of 37%;  $p < 0.05$ ) and glycolytic capacity (an average of 57%;  $p < 0.05$ ).

We next examined if GLUT3-forced expression could also impact the cytokines secretion by T cells. The latter, co-transduced with MART1-specific TCR and either NGFR (control) or GLUT3, were co-cultured with tumor targets. We observed a slight but significant increase in TNF- $\alpha$  and IFN- $\gamma$  secretion ranging from 15% to 70%, compared with NGFR control ([figure 5F,G](#)). These results indicate



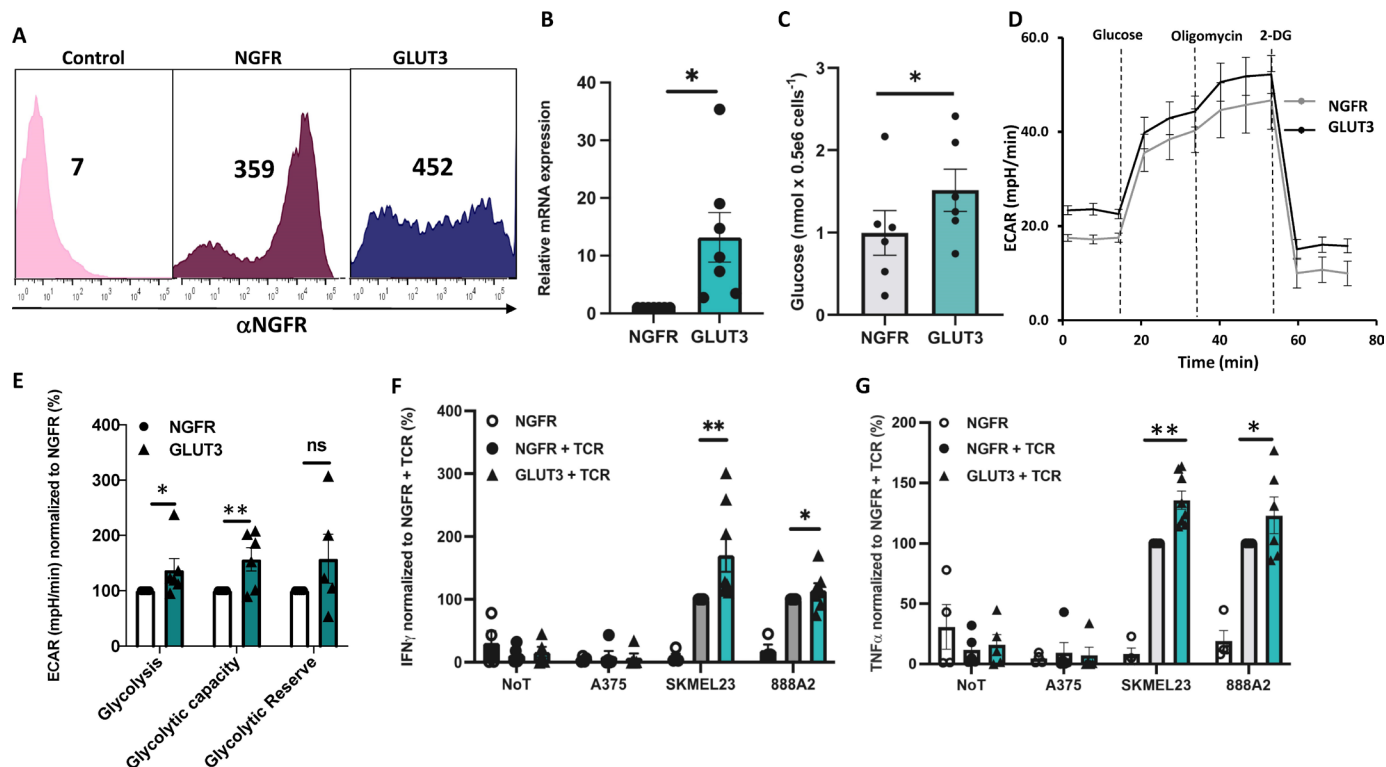


**Figure 5** GLUT3 transporter forced expression enhances glucose uptake and function in T cells. (A) Primary human PBLs were transduced with the retroviral vectors encoding GLUT3-I-NGFR or NGFR (control). 72 hours after transduction, expression was measured by flow cytometry using an antibody specific for NGFR ( $\alpha$ NGFR). The MFI values of positive cells are shown. These results are representative of at least five independent experiments with at least three different donors. The difference between the population transduced and the non-transduced population was found statistically significant ( $*p < 0.05$ ; calculated using a Student's paired t-test). (B) GLUT3 transcript expression was measured by quantitative PCR. These expression levels were normalized to the level of NGFR T cells (control). These results are presented as mean+SEM of 7 independent experiments performed with six different donors. The difference was found statistically significant ( $*p < 0.05$  as indicated, using a Student's paired t-test). (C) Glucose intracellular levels were measured using a glucose assay kit. These results are presented as mean+SEM of 6 independent experiments with different donors. A significant difference was observed between NGFR-overexpressing (control) and GLUT3-overexpressing T cells ( $*p < 0.05$  using a Student's paired t-test). (D–E) Evaluation of T-cell metabolic function by the Seahorse extracellular flux analyzer. Extracellular acidification rate (ECAR) was measured. (D) Depicts a representative experiment ( $n=8$  replicates). (E) Depicts the mean+SEM of 5 independent experiments performed with five different donors, normalized to control NGFR (with an average value of 25.3, 37.7 and 14.9 mpH/min for the glycolysis, glycolytic capacity and reserve, respectively). The difference between NGFR vector (control) and GLUT3 group was found statistically significant for the glycolysis rate and the glycolytic capacity as indicated ( $*p < 0.05$ , respectively, calculated using a Student's paired t-test). (F–G) Primary human T cells were transduced with a MART1-specific TCR and either NGFR (control) and GLUT3. These cells were co-cultured with cell lines as indicated (SKMEL23 or 888/A2) and negative control (A375) or no target. TNF- $\alpha$  (F) and IFN- $\gamma$  (G) secreted in the co-culture supernatant were measured by ELISA. These results are represented as the mean+SEM of at least three independent experiments performed with three different donors. The results were normalized to that obtained in the NGFR+TCR group (with reference concentrations ranging between 3.7 and 3.9 ng/mL for TNF- $\alpha$  and 2.7–4.6 ng/mL for IFN- $\gamma$ ). The difference between NGFR vector (control) and GLUT3 groups was found statistically significant as indicated ( $**p < 0.01$  and  $*p < 0.05$  calculated using a Student's paired t-test). GLUT3, glucose transporter 3; IFN, interferon; PBL, peripheral blood lymphocyte; MFI, mean fluorescence intensity; mRNA, messenger RNA; NGFR, nerve growth factor receptor; TCR, T-cell receptor; TNF, tumor necrosis factor.

that forced expression of GLUT3 may increase glucose uptake, glycolysis, and cytokine secretion by T cells.

### Combining PFK and GLUT3 improves T-cell metabolic functions and reduces exhaustion markers expression

After noting the favorable profile of PFK-transduced or GLUT3-transduced T cells, we moved to co-express them and assess the potential benefit of their simultaneous expression using a retroviral vector (PFK-IRES-GLUT3). This vector was used to transduce primary human T

cells. We detected an increase in the proportion of cells expressing PFK in the PFK-I-GLUT3 group (MFI=1126) compared with NGFR only (MFI=357; [figure 6A](#)). In parallel, we assessed PFK and GLUT3 transcript levels using quantitative PCR. We confirmed that RNA expression of PFK and GLUT3 was 6 and 17 times higher in PFK-I-GLUT3-transduced T cells than in the NGFR control ([figure 6B](#)). Similar to what was observed with PFK only ([figure 2B](#)), a significant increase was noted in



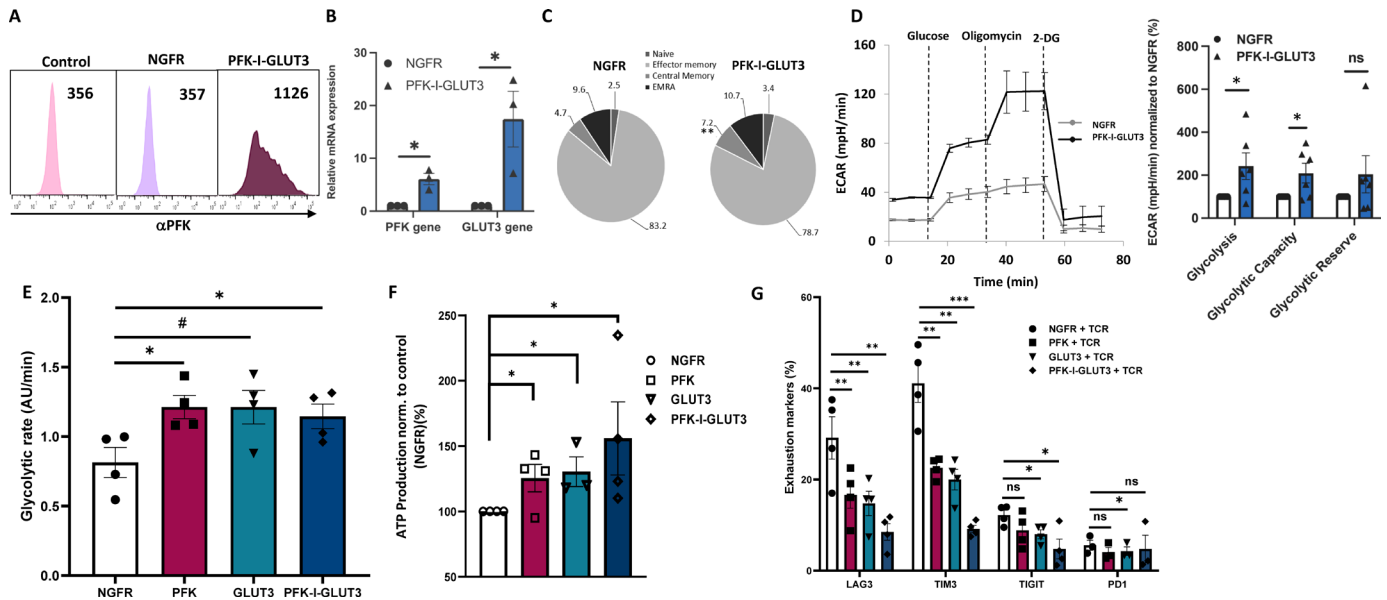


**Figure 6** PFK-IRES-GLUT3 improves T cells' metabolic functions and reduces exhaustion markers expression. (A–B) Primary human T cells were transduced with retroviral vectors encoding PFK-IRES-GLUT3 or NGFR. 72 hours after transduction, PFK expression was measured by flow cytometry. The MFI values of positive cells are shown. These results are representative of at least five independent experiments with at least five different donors. The difference between the population transduced and the non-transduced population was found statistically significant ( $*p < 0.05$ ; calculated using a Student's paired t-test). (B) PFK and GLUT3 transcript expression was measured by quantitative PCR. These expression levels were normalized to the level of NGFR T cells (control). These results are presented as mean+SEM of 3 independent experiments performed with three different donors. The difference was found to be statistically significant ( $*p < 0.05$  as indicated, using a Student's paired t-test). (C) The memory phenotype of transduced cells was determined by flow cytometry based on CD45RO and CCR7 expression. These results are presented as the mean of 6 independent experiments with three different donors. The percentage of central memory cells was statistically significant between NGFR (control group) and PFK-I-GLUT3 ( $**p < 0.01$ , using a Student's paired t-test). (D) Evaluation of T-cell metabolic function by the Seahorse extracellular flux analyzer. Extracellular acidification rate (ECAR) was measured. The left panel depicts a representative experiment ( $n=8$  replicates). The right panel depicts the mean+SEM of 6 independent experiments performed with five different donors, normalized to control NGFR (with an average value of 27.9, 40.4 and 12.5 mpH/min for the glycolysis, glycolytic capacity and reserve, respectively). The difference between NGFR vector (control) and PFK-I-GLUT3 group was found statistically significant for glycolysis rate and the glycolytic capacity as indicated ( $*p < 0.05$ , calculated using a Student's paired t-test). (E) ATP levels were measured using the CellTiter-Glo 2.0 Cell Viability Assay ATP measurement kit reagent that was added to  $1 \times 10^5$  T cells in a 96-well plate. The ATP expression levels were normalized to the control (NGFR—248,322 RLU). These results are representative of four independent experiments performed with four donors. The difference between PFK, GLUT3, PFK-I-GLUT3 and NGFR (control) was found statistically significant as indicated ( $*p < 0.05$ , calculated using a Student's paired t-test). (F) PFK, GLUT3, PFK-I-GLUT3 and NGFR engineered T cells were stained for LAG3, TIM3, TIGIT and PD-1 expression which was measured by flow cytometry. These results are presented as the mean+SEM of at least three independent experiments with three different donors (a representative staining assay is presented in online supplemental figure 2). GLUT3, glucose transporter 3; LAG3, lymphocyte activation gene 3; MFI, mean fluorescence intensity; NGFR, nerve growth factor receptor; PBL, peripheral blood lymphocyte; PD-1, programmed cell death protein 1; PFK, phosphofructokinase; TCR, T-cell receptor; TIGIT, T cell immunoreceptor with Ig and ITIM domains; TIM-3, T-cell immunoglobulin and mucin-domain containing-3; TNF, tumor necrosis factor.

the distribution of the central memory population in the PFK-I-GLUT3 versus NGFR groups (7.2% compared with 4.7%;  $p < 0.01$ , figure 6C).

As above, we tested the glycolytic function of PFK-I-GLUT3 T cells (figure 6D). Compared with the NGFR control, we noted in the PFK-I-GLUT3 an increase in glycolysis (with an average of 242%;  $p < 0.05$ ) and a superior glycolytic capacity (with an average of 210%;  $p < 0.05$ ). This trend was further confirmed when using a glycolysis rate assay kit (figure 6E). We also measured ATP levels in PFK, GLUT3, PFK-I-GLUT3 or NGFR-transduced T cells (figure 6F) and noted a 25%, 30% and 56% increase

respectively in the treated groups compared with control ( $p < 0.05$ ).

As previously mentioned, TME conditions can often hinder T-cell survival and effector functions, leading to a state of exhaustion.<sup>27</sup> Thus, we measured the expression of exhaustion markers (lymphocyte activation gene 3 (LAG3), T-cell immunoglobulin and mucin-domain containing-3 (TIM3), T cell immunoreceptor with Ig and ITIM domains (TIGIT) and programmed cell death protein 1 (PD-1)) in NGFR, PFK, GLUT3 and PFK-IRES-GLUT3-engineered T cells. We mostly observed a lower LAG3, TIM3, TIGIT and PD-1 expression in the PFK,

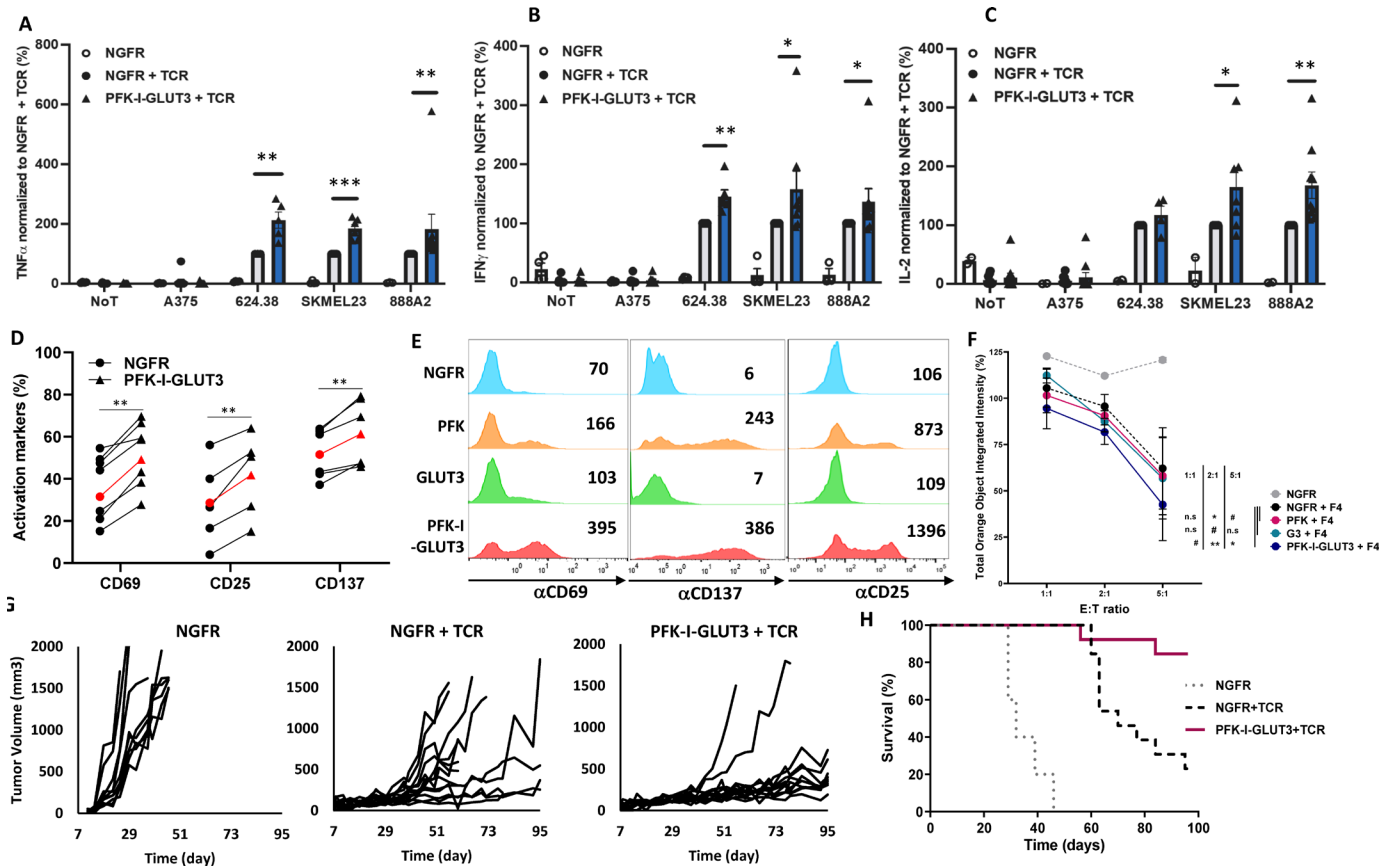


**Figure 7** PFK-IRES-GLUT3 improves T-cell antitumor function in vitro and in vivo. (A–C) Transduced PBLs expressing MART1-specific TCR receptor were co-cultured with 624.38, SKMEL23 and 888/A2 as positive controls and A375 cell line as negative control or without targets (NoT). TNF- $\alpha$  (A) IFN- $\gamma$  (B) and IL-2 (C) secreted in the co-culture supernatant were measured by ELISA. These results represent the mean+SEM of at least four independent experiments performed with at least three different donors. The results were normalized to NGFR+TCR (with reference concentrations ranging between 0.4 and 2.4 ng/mL for TNF- $\alpha$ , 0.6–5.9 ng/mL for IFN- $\gamma$  and 0.13 to 1.3 ng/mL for IL-2). The difference between NGFR vector (control) and PFK-I-GLUT3 was found statistically significant as indicated (\*\* $p < 0.001$  to \* $p < 0.05$  calculated using a Student's paired t-test). (D–E) CD69, CD25, and CD137 expression were measured by flow cytometry, gated on the CD8+ population. (D) The results are at least five independent experiments performed with at least three different donors. (E) Representative results of stimulated engineered-T cells for each group and each marker are shown. (F) NGFR, NGFR+F4, PFK+F4, GLUT3+F4 and PFK-I-GLUT3+F4 were co-cultured with tumor cells (888A2) at different E:T (effector:target) ratio and incubated in an IncuCyte apparatus. Live cells mCherry<sup>+</sup> population over time was normalized to t=0. These results are the mean+SEM of 3 independent experiments performed with at least three different donors. The difference between NGFR vector (control) and PFK-I-GLUT3 was found statistically significant as indicated (calculated using a Student's paired t-test). (G) NSG mice inoculated with  $2 \times 10^6$  888/A2 tumor cells.  $5 \times 10^6$  of NGFR+TCR or PFK-I-GLUT3 + TCR-engineered T cells were intravenous injected in mice, 1 week and 2 weeks after tumor establishment. Tumor growth was measured in a blinded fashion using a caliper and calculated using the following formula:  $(D \times d^2) \times \pi / 6$ , where D is the largest tumor diameter and d is its perpendicular diameter. Spider plots of the tumor volumes are shown (G) and the survival is represented by a Kaplan-Meier curve (H). The difference between the PFK-I-GLUT3 + TCR and NGFR+TCR treated groups was found statistically significant (LogRank test; \*\* $p < 0.002$ ). GLUT3, glucose transporter 3; IFN, interferon; IL, interleukin; NGFR, nerve growth factor receptor; PFK, phosphofruktokinase; TCR, T-cell receptor; TNF, tumor necrosis factor.

GLUT3 and PFK-I-GLUT3 group compared with the control NGFR groups (1.75–3.43 times lower for LAG3, 1.8–4.48 for TIM3, 1.38–2.55 for TIGIT and 1.4–0.2 for PD-1 expression figure 6G and online supplemental figure 2). Overall, T cells engineered to express PFK concomitantly with GLUT3 exhibited a lower expression of inhibitory markers and higher glycolysis levels.

### PFK-IRES-GLUT3 improves T-cell antitumor function in vitro and in vivo

Following our previous results, we tested the function of PFK-I-GLUT3-engineered cells. We co-cultured MART1-specific TCR-T cells engineered with either PFK-I-GLUT3 or NGFR and cancer cells. Following this, we measured TNF- $\alpha$ , IFN- $\gamma$ , and IL-2 secretion in the supernatant. In general, we observed an increased secretion of these cytokines by PFK-I-GLUT3. For example, in co-culture with 624.38, PFK-I-GLUT3-T cells secreted more than

twice TNF- $\alpha$  than the control NGFR (222% vs 100% in figure 7A,  $p < 0.01$ , with an average of 400 pg/mL in the control group) and 1.5 more IFN- $\gamma$  ( $p < 0.05$ ) in co-cultures with SKMEL23. No significant cytokine secretion was noted in co-cultures with T cells engineered only with metabolic constructs (ie, untransduced with TCR – online supplemental figure 3). We also tested the expression of activation markers (CD69, CD137, and CD25; figure 7D–F) and generally noted an increase in the PFK-I-GLUT3 population compared with control NGFR. For example, we observed 59% more expression of CD69 in the PFK-I-GLUT3 group compared with control ( $p < 0.01$ ). Furthermore, in co-cultures 888A2 and 624.38, we noted an upregulation of CD107a on the NGFR positive populations (ie, expressing the metabolic transgenes) with, for example, a proportion of 21.6–24.6% positive cells compared with 14.8% for the NGFR-only control group for CD107a in co-cultures with the 888A2 cell line (online supplemental figure 4A,B,  $p < 0.001$ ). We additionally measured CD69 in engineered T cells after an overnight co-culture with 888A2 and 624.38 cell lines and observed between 1.5 and 2.4 times more CD69 expression in all the groups compared with the NGFR-only control group (online supplemental figure 4C,D,  $p < 0.01$ ).

We then measured cell-mediated cytotoxicity and observed a significantly lower percentage of live melanoma target cells following co-culture with PFK-I-GLUT3-engineered T cells compared with control at different E:T ratios (figure 7F). No significant cytotoxicity was observed against antigen-negative control melanoma target A375 or with NGFR without TCR (online supplemental figure 5).

Finally, we assessed the *in vivo* antitumor function of PFK-I-GLUT3-transduced T cells and examined the ability of the latter to delay tumor growth in a human tumor xenograft mouse model. For this purpose,  $2 \times 10^6$  tumor cells (888/A2) were injected into the flank of NSG mice.  $5 \times 10^6$  T cells (PFK-I-GLUT3 + TCR or NGFR+TCR) were injected through the tail vein 1 and 2 weeks after the tumor cell injection. We followed tumor growth and noted that PFK-I-GLUT3 + TCRT cells mediated a significant delay in tumor growth compared with the control group that was treated with NGFR+MART1-specific TCR-transduced T cells (figure 7G;  $n = 13$ ,  $p < 0.01$ ). Moreover, at the experiment endpoint, 84% of the PFK-I-GLUT3-treated mice survived compared with 23% in the control group (figure 7H,  $p = 0.002$  by LogRank analysis). In conclusion, PFK-I-GLUT3-overexpressing T cells could delay tumor growth and significantly prolong the survival of tumor-bearing mice.

## DISCUSSION

In this study, we show that it is possible to genetically engineer T cells to express genes linked to the glycolysis pathway, namely PFK and GLUT3, to improve their antitumor function.

Several studies have underscored the low concentrations of glucose in the TME compared with plasma<sup>28</sup> or in the interstitial fluid of advanced tumors.<sup>29</sup> Glucose is crucial to the antitumor function, and its depletion can lead to drastically dampened T-cell proliferation, cytokine production, and cytotoxicity,<sup>30</sup> impairing an effective immune response against the tumor. Most studies demonstrated the limited availability of glucose to T cells in the TME,<sup>31</sup> though a recent study also showed that tumor-infiltrating T cells may harness similar amounts of glucose compared with tumor cells, but these lymphocytes still exhibited defective glycolysis.<sup>32</sup> Nonetheless, a recent study by Zhu *et al*<sup>33</sup> showed that T cells stimulated and cultured in high glucose conditions demonstrated a higher glycolysis rate and cytotoxic potential. The latter is important, as we observed that augmenting glucose transport to engineered T cells could bolster their glycolytic capacity (figure 5). We also noted an increase in lactate production by PFK-engineered cells. This metabolite is known to play a crucial role in shaping the immune response in the TME. On the one hand, it was shown that lactate may serve as a fuel source for tumor cells and increase their survival.<sup>34</sup> It might be valuable in the present context to study the potential benefit of parallel strategies targeting lactate such as the use of MCT inhibitors.<sup>35</sup> Though some reports have shown that lactate might attenuate T-cell function,<sup>34</sup> recent studies have shown that it could improve T cells' antitumor activity and preserve their stemness.<sup>36 37</sup>

In the present report, we chose to specifically focus on two glycolysis-linked components: PFK, which is a rate-limiting glycolysis enzyme, and GLUT3, displaying among different transporters the highest affinity for glucose.<sup>38</sup> Tumor cells also seem to partly use similar strategies to cope with the harsh nutrient conditions in the microenvironment that they themselves contribute to generating by also upregulating both PFK and GLUT3.<sup>25 39</sup> Alternatively, glycolytic activity in T cells can, in general, fuel autoimmune syndromes,<sup>31 40</sup> and both these proteins were also implicated in T-cell overactivity and the exacerbation of diseases.<sup>40–42</sup> For example, a recent study demonstrated that GLUT3 controls the T-cell inflammatory response in models of autoimmune colitis and encephalomyelitis.<sup>42</sup> In the context of the antitumor response, an autoimmune-like activity against tumor cells would be desirable. Moreover, our present report confirms and extends a recent study by Coukos and colleagues<sup>43</sup> that showed in a mouse model that overexpression of GLUT3 can improve T-cell antitumor activity. Similarly, in our human system, we confirmed that glucose uptake, and cytokine secretion improved in GLUT3-engineered human T cells (figure 5).

Additionally, it was shown that inhibition of glycolysis in T cells might contribute to exhaustion.<sup>44</sup> Conversely, we showed herein that cells engineered to express PFK-I-GLUT3 displayed lower levels of LAG3, TIM3, TIGIT and PD-1 (figure 6F), thus alleviating the exhaustion phenotype of T cells. This is of interest as it was shown that checkpoint ligation such as PD-1 can inhibit glycolysis in T



cells.<sup>45</sup> Thus, one may surmise that the present strategy of boosting glycolysis in T cells not only provides increased energy but also may contribute to lower secondary glycolysis inhibition orchestrated by checkpoint molecules.<sup>44</sup>

ATP can act as an allosteric inhibitor of PFK, which raises questions about how increased ATP levels may affect PFK activity and subsequently glycolytic flux in T cells. However, it is important to consider the context-dependent nature of ATP regulation in T cells. While high ATP levels may inhibit PFK activity under certain conditions, T-cell activation and effector function often require rapid ATP production to support energy-demanding processes such as proliferation and cytokine production. Therefore, the relationship between ATP levels and PFK activity may be dynamic and finely tuned to meet the metabolic demands of activated T cells.<sup>46</sup>

This study is mainly focused on a well characterized and clinically relevant TCR/melanoma model.<sup>47</sup> Although melanoma tumors are known to be glycolytic,<sup>48</sup> it will be important to confirm that our present approach might be particularly advantageous in the context of other solid tumors, as the most glycolytic tumor types are often aggressive and highly proliferative,<sup>49</sup> like in the case triple-negative breast cancer. Other highly glycolytic tumor types include pancreatic cancer, lung cancer, and glioblastoma. Also, as in many T-cell engineering studies, we used T cells derived from healthy donors; it will be relevant in subsequent studies to extend this approach to lymphocytes derived from patients with cancer. Our strategy may also provide a competitive advantage not only against tumor cells but also against other resident cells, such as those from the myeloid lineage, which were found to scavenge most glucose in the TME.<sup>32</sup>

Different strategies may impact T-cell immunometabolism to enhance their function and therapeutic purposes, including using the targeted delivery of metabolic modulators in the TME or, alternatively, to precondition T cells in different medium or growing conditions prior to transfer.<sup>50</sup> These approaches may be limited, as T cells might revert to their previous phenotype after adoptive transfer, or modulators may display off-target effects and require repetitive treatments.

Using genetically modified T cells allows for bypassing some of these limitations and generating stably enhanced effector T cells. The present approach may be readily implemented in clinical trials and could be extended to other key components of glycolysis and/or metabolic pathways to enhance the activity of tumor-specific T cells, whether CAR/TCR engineered, naturally occurring like TILs, or even in other types of white blood cells like B or natural killer lymphocytes, for therapeutic purposes. For example, it was shown that the weakened activity of enolase, another important enzyme for glycolysis, dampens CD8+TIL antitumor function.<sup>51</sup> By controlling the rate of glycolysis, PFK indirectly influences mitochondria and affects the availability of substrates (such as pyruvate) that enter the mitochondria for further metabolism. Mitochondria activity is crucial for CD8

T-cell function in antitumor immunity and contribute to energy production, reactive oxygen species (ROS) levels regulation and memory formation. Thus, the present approach might also be compatible with mitochondrial functional enhancements. For example, it was shown that engineering CD8+T cells to express PGC1 $\alpha$ , a pivotal controller of mitochondrial biogenesis, bolstered their antitumor activity by rescuing mitochondrial function.<sup>52</sup> Other strategies could be directed to influence the hypoxia response<sup>53</sup> or amino acid synthesis pathways; for example, CAR T-cell overexpressing arginosuccinate synthase and ornithine transcarboxylase exhibited enhanced clearance of tumors.<sup>54</sup>

In summary, we have demonstrated that enforced expression of the PFK enzyme and the glucose transporter GLUT3 supports the metabolic fitness of T cells and increases their function both in vitro and in vivo. We are confident that this approach geared at immunometabolism manipulation bears important implications for enhancing immune cell-based therapies.

**Acknowledgements** We want to thank Dr Jennifer Benichou Israel Cohen from the statistical unit in the Faculty of Life Sciences, Bar-Ilan University for her advice on statistical data processing and presentation. We thank Ms Riki Sabbag for her technical help in executing in vivo experiments work and Ms Yael Laure for editing the manuscript.

**Contributors** Conceptualization: CJC, RTZ; Methodology: OA, TB, IA; Investigation: RTZ, OA, SH; Funding acquisition: CJC; Supervision: CJC, NR-H, EG; Writing—original and revised draft: RTZ, CJC. Guarantor: CJC.

**Funding** This work was supported by the Adelis Foundation, the Israel Science Foundation (646/20) and the Koarsa Cancer Research Institute. We thank the Joseph Wybran Lodge of Bnai Brith France for awarding RTZ the prize in immunology and cancer research.

**Competing interests** We declare that CJC, RTZ and TB are inventors on a submitted PCT Application No. PCT/IL2023/050248 related to this study. All other authors declare that they have no competing interests.

**Patient consent for publication** Not applicable.

**Ethics approval** Not applicable.

**Provenance and peer review** Not commissioned; externally peer reviewed.

**Data availability statement** Data are available upon reasonable request.

**Supplemental material** This content has been supplied by the author(s). It has not been vetted by BMJ Publishing Group Limited (BMJ) and may not have been peer-reviewed. Any opinions or recommendations discussed are solely those of the author(s) and are not endorsed by BMJ. BMJ disclaims all liability and responsibility arising from any reliance placed on the content. Where the content includes any translated material, BMJ does not warrant the accuracy and reliability of the translations (including but not limited to local regulations, clinical guidelines, terminology, drug names and drug dosages), and is not responsible for any error and/or omissions arising from translation and adaptation or otherwise.

**Open access** This is an open access article distributed in accordance with the Creative Commons Attribution Non Commercial (CC BY-NC 4.0) license, which permits others to distribute, remix, adapt, build upon this work non-commercially, and license their derivative works on different terms, provided the original work is properly cited, appropriate credit is given, any changes made indicated, and the use is non-commercial. See <http://creativecommons.org/licenses/by-nc/4.0/>.

**ORCID iD**

Cyrille J Cohen <http://orcid.org/0000-0002-0619-5959>



## REFERENCES

- 1 Kist de Ruijter L, van de Donk PP, Hoiveld-Noeken JS, *et al.* Whole-body Cd8(+) T cell visualization before and during cancer Immunotherapy: a phase 1/2 trial. *Nat Med* 2022;28:2601–10.
- 2 Finck AV, Blanchard T, Roselle CP, *et al.* Engineered cellular Immunotherapies in cancer and beyond. *Nat Med* 2022;28:678–89.
- 3 Ribas A, Wolchok JD. Cancer Immunotherapy using Checkpoint blockade. *Science* 2018;359:1350–5.
- 4 Eisenberg V, Hoogi S, Shamul A, *et al.* “T-cells “a La CAR-T(E)” - genetically engineering T-cell response against cancer”. *Advanced Drug Delivery Reviews* 2019;141:23–40.
- 5 Baker DJ, Arany Z, Baur JA, *et al.* CAR T therapy beyond cancer: the evolution of a living drug. *Nature* 2023;619:707–15.
- 6 Harush O, Asherie N, Kfir-Erenfeld S, *et al.* Preclinical evaluation and structural optimization of anti-BCMA CAR to target multiple myeloma. *Haematologica* 2022;107:2395–407.
- 7 Zur RT, Adler G, Shamalov K, *et al.* Adoptive T-cell Immunotherapy: perfecting self-defenses. *Exp Suppl* 2022;113:253–94.
- 8 Aksoylar H-I, Tijaro-Ovalle NM, Boussiatis VA, *et al.* T cell metabolism in cancer Immunotherapy. *Immunometabolism* 2020;2:e200020.
- 9 Asherie N, Kfir-Erenfeld S, Avni B, *et al.* Development and manufacturing of novel locally produced anti-BCMA CART cells for the treatment of Relapsed/refractory multiple myeloma: phase I clinical results. *Haematol* 2022;108:1827–39.
- 10 Elia I, Haigis MC. Metabolites and the tumour Microenvironment: from cellular mechanisms to systemic metabolism. *Nat Metab* 2021;3:21–32.
- 11 Menk AV, Scharping NE, Moreci RS, *et al.* Early TCR signaling induces rapid aerobic Glycolysis enabling distinct acute T cell Effector functions. *Cell Rep* 2018;22:1509–21.
- 12 Siska PJ, Rathmell JC. Metabolic signaling drives IFN-gamma. *Cell Metab* 2016;24:651–2.
- 13 Ho P-C, Bihuniak JD, Macintyre AN, *et al.* Phosphoenolpyruvate is a metabolic Checkpoint of anti-tumor T cell responses. *Cell* 2015;162:1217–28.
- 14 Chapman NM, Boothby MR, Chi H. Metabolic coordination of T cell quiescence and activation. *Nat Rev Immunol* 2020;20:55–70.
- 15 Yi W, Clark PM, Mason DE, *et al.* Phosphofructokinase 1 Glycosylation regulates cell growth and metabolism. *Science* 2012;337:975–80.
- 16 Halperin ML, Connors HP, Reiman AS, *et al.* Factors that control the effect of pH on Glycolysis in leukocytes. *J Biol Chem* 1969;244:384–90.
- 17 Hue L, Rider MH. Role of fructose 2,6-Bisphosphate in the control of Glycolysis in mammalian tissues. *Biochem J* 1987;245:313–24.
- 18 Haga-Friedman A, Horovitz-Fried M, Cohen CJ. Incorporation of Transmembrane hydrophobic mutations in the TCR enhance its surface expression and T cell functional avidity. *J Immunol* 2012;188:5538–46.
- 19 Bettinotti MP, Kim CJ, Lee KH, *et al.* Stringent allele/EPITOPE requirements for MART-1/Melan A Immunodominance: implications for peptide-based Immunotherapy. *J Immunol* 1998;161:877–89.
- 20 Eisenberg V, Hoogi S, Shamul A, *et al.* “T-cells “a La CAR-T(E)” - genetically engineering T-cell response against cancer”. *Adv Drug Deliv Rev* 2019;141:23–40.
- 21 Zheng Z, Chinnasamy N, Morgan RA. Protein L: a novel reagent for the detection of Chimeric antigen receptor (CAR) expression by flow Cytometry. *J Transl Med* 2012;10:29.
- 22 Zuo J, Tang J, Lu M, *et al.* Glycolysis rate-limiting enzymes: novel potential regulators of rheumatoid arthritis pathogenesis. *Front Immunol* 2021;12:779787.
- 23 Cohen CJ, Li YF, El-Gamil M, *et al.* Enhanced antitumor activity of T cells engineered to express T-cell receptors with a second Disulfide bond. *Cancer Res* 2007;67:3898–903.
- 24 Hoogi S, Eisenberg V, Mayer S, *et al.* A TIGIT-based Chimeric Co-stimulatory switch receptor improves T-cell anti-tumor function. *J Immunother Cancer* 2019;7:243.
- 25 Pliszka M, Szablewski L. Glucose transporters as a target for anticancer therapy. *Cancers (Base)* 2021;13:4184.
- 26 Burant CF, Bell GI. Mammalian Facilitative glucose transporters: evidence for similar substrate recognition sites in functionally monomeric proteins. *Biochemistry* 1992;31:10414–20.
- 27 Lim AR, Rathmell WK, Rathmell JC. The tumor Microenvironment as a metabolic barrier to Effector T cells and Immunotherapy. *Elife* 2020;9:e55185.
- 28 Sullivan MR, Danai LV, Lewis CA, *et al.* Quantification of Microenvironmental metabolites in murine cancers reveals determinants of tumor nutrient availability. *Elife* 2019;8:e44235.
- 29 Cortese S, Morales J, Martín L, *et al.* Hepatic resection with Thrombectomy in the treatment of hepatocellular carcinoma associated with Macrovascular invasion. *Cirugía Española (English Edition)* 2020;98:9–17.
- 30 Konjar Š, Veldhoen M. Dynamic metabolic state of tissue resident Cd8 T cells. *Front Immunol* 2019;10:1683.
- 31 Chapman NM, Chi H. Metabolic adaptation of lymphocytes in immunity and disease. *Immunity* 2022;55:14–30.
- 32 Reinfield BI, Madden MZ, Wolf MM, *et al.* Cell-programmed nutrient partitioning in the tumour Microenvironment. *Nature* 2021;593:282–8.
- 33 Zhu J, Yang W, Zhou X, *et al.* High glucose enhances cytotoxic T lymphocyte-mediated cytotoxicity. *Front Immunol* 2021;12:689337.
- 34 Li Z, Wang Q, Huang X, *et al.* Lactate in the tumor Microenvironment: A rising star for targeted tumor therapy. *Front Nutr* 2023;10:1113739.
- 35 Lopez E, Karatill R, Nannini F, *et al.* Inhibition of lactate transport by MCT-1 blockade improves Chimeric antigen receptor T-cell therapy against B-cell malignancies. *J Immunother Cancer* 2023;11:e006287.
- 36 Feng Q, Liu Z, Yu X, *et al.* Lactate increases Stemness of Cd8 + T cells to augment anti-tumor immunity. *Nat Commun* 2022;13:4981.
- 37 Barbieri L, Veliça P, Gameiro PA, *et al.* Lactate exposure shapes the metabolic and Transcriptomic profile of Cd8+ T cells. *Front Immunol* 2023;14:1101433.
- 38 Custódio TF, Paulsen PA, Frain KM, *et al.* Structural comparison of Glut1 to Glut3 reveal transport regulation mechanism in sugar Porter family. *Life Sci Alliance* 2021;4:e202000858.
- 39 Shen J, Jin Z, Lv H, *et al.* PFKF is highly expressed in lung cancer and regulates glucose metabolism. *Cell Oncol (Dordr)* 2020;43:617–29.
- 40 Xu K, Yin N, Peng M, *et al.* Glycolytic ATP fuels Phosphoinositide 3-kinase signaling to support Effector T helper 17 cell responses. *Immunity* 2021;54:976–87.
- 41 Scherlinger M, Pan W, Hisada R, *et al.* Phosphofructokinase P fine-tunes T regulatory cell metabolism, function, and stability in systemic Autoimmunity. *Sci Adv* 2022;8:eadc9657.
- 42 Hochrein SM, Wu H, Eckstein M, *et al.* The glucose transporter Glut3 controls T helper 17 cell responses through Glycolytic-epigenetic Reprogramming. *Cell Metab* 2022;34:516–32.
- 43 Cribioli E, Giordano Attianese GMP, Ginefra P, *et al.* Enforcing Glut3 expression in Cd8(+) T cells improves fitness and tumor control by promoting glucose uptake and energy storage. *Front Immunol* 2022;13:976628.
- 44 Martins CP, New LA, O'Connor EC, *et al.* Glycolysis inhibition induces functional and metabolic exhaustion of Cd4(+) T cells in type 1 diabetes. *Front Immunol* 2021;12:669456.
- 45 Patsoukis N, Bardhan K, Chatterjee P, *et al.* PD-1 alters T-cell metabolic Reprogramming by inhibiting Glycolysis and promoting Lipolysis and fatty acid oxidation. *Nat Commun* 2015;6:6692.
- 46 Yang Z, Fujii H, Mohan SV, *et al.* Phosphofructokinase deficiency impairs ATP generation, Autophagy, and redox balance in rheumatoid arthritis T cells. *J Exp Med* 2013;210:2119–34.
- 47 Morgan RA, Dudley ME, Wunderlich JR, *et al.* Cancer regression in patients after transfer of genetically engineered lymphocytes. *Science* 2006;314:126–9.
- 48 Neagu M. Metabolic traits in cutaneous Melanoma. *Front Oncol* 2020;10:851.
- 49 Cohen IJ, Pareja F, Succi ND, *et al.* Increased tumor Glycolysis is associated with decreased immune infiltration across human solid tumors. *Front Immunol* 2022;13:880959.
- 50 Corrado M, Pearce EL. Targeting memory T cell metabolism to improve immunity. *J Clin Invest* 2022;132:e148546.
- 51 Gemta LF, Siska PJ, Nelson ME, *et al.* Impaired Enolase 1 Glycolytic activity restrains Effector functions of tumor-infiltrating Cd8(+) T cells. *Sci Immunol* 2019;4:eaap9520.
- 52 Scharping NE, Menk AV, Moreci RS, *et al.* The tumor Microenvironment represses T cell mitochondrial Biogenesis to drive Intratumoral T cell metabolic insufficiency and dysfunction. *Immunity* 2016;45:374–88.
- 53 Kostı P, Opzomer JW, Larios-Martinez KI, *et al.* Hypoxia-sensing CAR T cells provide safety and efficacy in treating solid tumors. *Cell Rep Med* 2021;2:100227.
- 54 Fultang L, Booth S, Yogev O, *et al.* Metabolic engineering against the arginine Microenvironment enhances CAR-T cell proliferation and therapeutic activity. *Blood* 2020;136:1155–60.